THE GEO-MECHANICS BEHAVIOR OF SOFT MARINE SILTS UNDER A NEARSHORE RUBBLE-MOUND BREAKWATER

LIEN-KWEI CHIEN, TSUNG-SHEN FENG and TSUNG-CHING CHEN

About the authors

Lien-kwei Chien
National Taiwan Ocean University,
Department of Harbor and River Engineering
No. 2 Pei-Ninig Road, Keelung 202, Taiwan
E-mail: lkchien@mail.ntou.edu.tw

Tsung-shen Feng
National Taiwan Ocean University,
Department of Harbor and River Engineering
No. 2 Pei-Ninig Road, Keelung 202, Taiwan
E-mail: D91520004@mail.ntou.edu.tw

Tsung-ching Chen
National Taiwan Ocean University,
Department of Harbor and River Engineering
No. 2 Pei-Ninig Road, Keelung 202, Taiwan
E-mail: M93520078@mail.ntou.edu.tw

Abstract

In this study, the soft marine silts under a rubble-mound breakwater in Ma-Zu of west Taiwan are adopted as a test sample. The specimens were prepared by a new, remolded method at dry density and consolidated stresses. Tri-axial shear-strength tests were performed to evaluate the pore-water pressure and the shear strength. The test results show that the pore-water pressure increases gradually and is close to the critical values as the axial strain increases. In addition, under isotropic and K_0 consolidation, both the c and c′ of the soft marine silts were 0 kPa, which means that the silts do not have any shear resistance, just like fluid under a rubble-mound breakwater. Based on the linear-elasticity and the one-dimensional consolidation theory, the model of the settlement and stability was evaluated in SIGMA/W. The results show that the soft marine silts at the breakwater induced a displacement, greatly increasing with the filling rubble-mound loading. The figures and results can be referenced for a stability evaluation of the silt soil deposits under the rubble-mound breakwater. The results are useful for marine silts mechanics and a stability analysis for the planning, design, and related research on near-shore engineering.

Keywords

geo-mechanics behavior, soft marine silt, rubble-mound breakwater, settlement, numerical simulation model

1 INTRODUCTION

In 1995, the geo-structure of the rubble-mound breakwater settled gradually during the construction of Beigan in Ma-Zu. The silt layer at the front section of the rubble-mound breakwater had heaved. When the breakwater at the Fuao Commercial Port of Nangan, Matzu was expanded in 2002, serious settlement and lateral displacement appeared during the construction. Meanwhile, marine silts caused the foundation settlement of near-shore structures due to the inferior nature of the works, and the settlement quantity is the variable that changes with time, due to unpredictable factors such as storm waves, which are the main reason for the cause of disasters to the shore and harbor engineering (Chien et al., 2007).

In 2005, the breakwater in the north dock named Bai-Sah in Ma-Zu County was extended. The actual amounts of mound were different from the original design. As a result, the extended harbor geo-structure stopped working properly.

Chen (2004) studied the topic of a mound breakwater by physical testing, micro-fabric analysis and mechanics properties, and evaluated the possible factors and stable mechanism. Chien et al. (2005) studied an improved model using the mixing method. Furthermore, the bearing capacity was promoted by using cement-mixed soft silt clay, which also increased the shear strength of the soft clay. Mayne et al. (1990) studied the specimen stress and the corresponding model of the field under different structural loadings.

In order to further discuss the disasters factor caused by marine silts, the ongoing expansion of the breakwaters at the Fuao Port of Ma-Zu was the research area in this study. A static experiment and a numerical analysis were performed to evaluate the factors causing the breakage

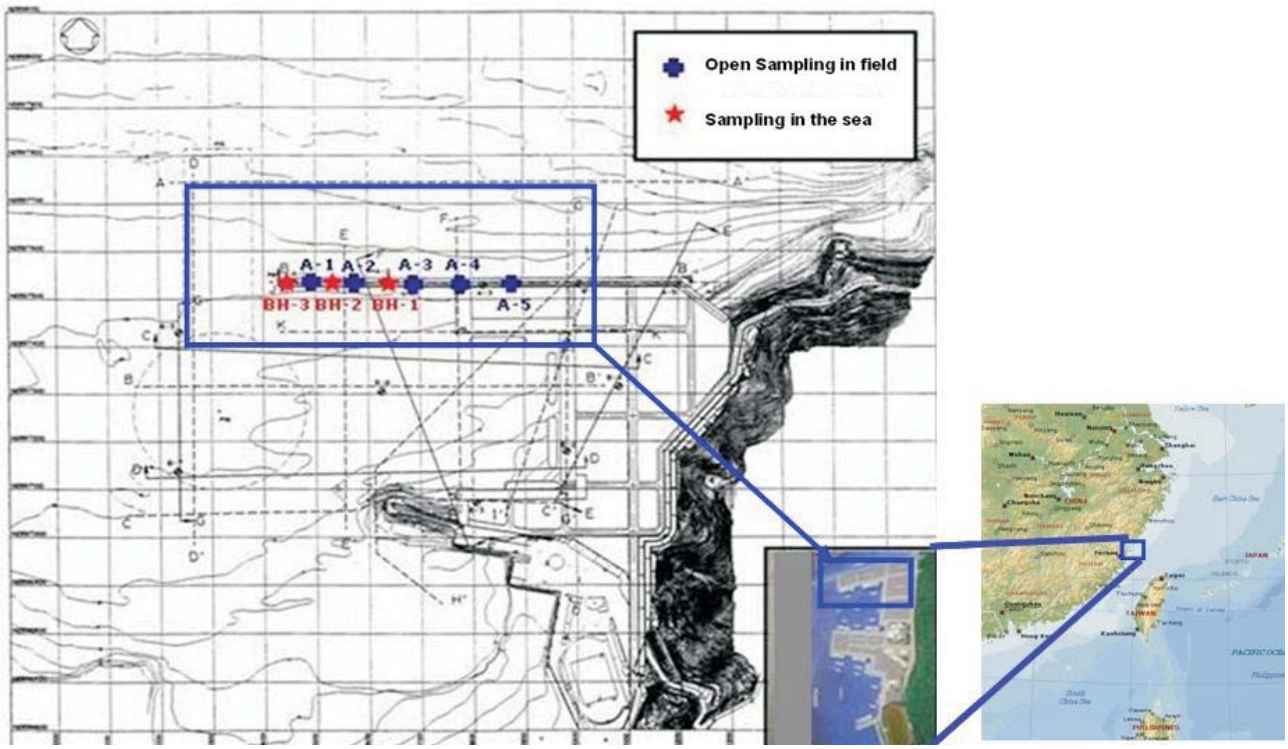

Figure 1. Locations of borings and soil sampling in the Ma-Zu extended breakwater.

of the rubble-mound breakwaters. The figures and the results can be referenced for the stability evaluation of silt soil deposits under the rubble-mound breakwater.

1.1 ANALYSIS OF RESEARCH AREA

Based on the near-shore exploration work, the locations of the borings and the soil sampling in Ma-Zu County are shown in Fig.1. From the near-shore exploration data, most of the mean SPT-N values of the profile below 12 m of the seabed were near 1, and a few of them were 7. The relationship between the SPT-N value and the depth of the exploration at the rubble-mound breakwaters are shown in Fig. 2.

1.2 BASIC PHYSICAL PROPERTIES OF THE SOIL

The liquid limit (LL) of the seabed soils at five different locations ranged from 42% to 47%, the plastic limit (PL) from 26% to 31%, and the plasticity index (PI) from 12% to 20%, based on the results of the Atterberg limit tests.

According to x-ray diffraction of the soft marine silts in Fuao, Matzu and the possible elements judged by EDS, the main chemical compositions of the soft marine

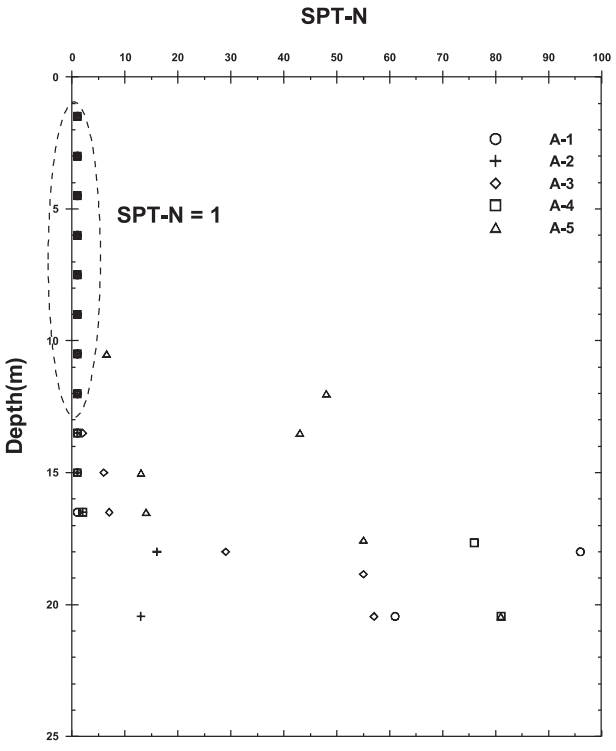

Figure 2. Relationship between the SPT-N value and the depth below the rubble-mound breakwater.

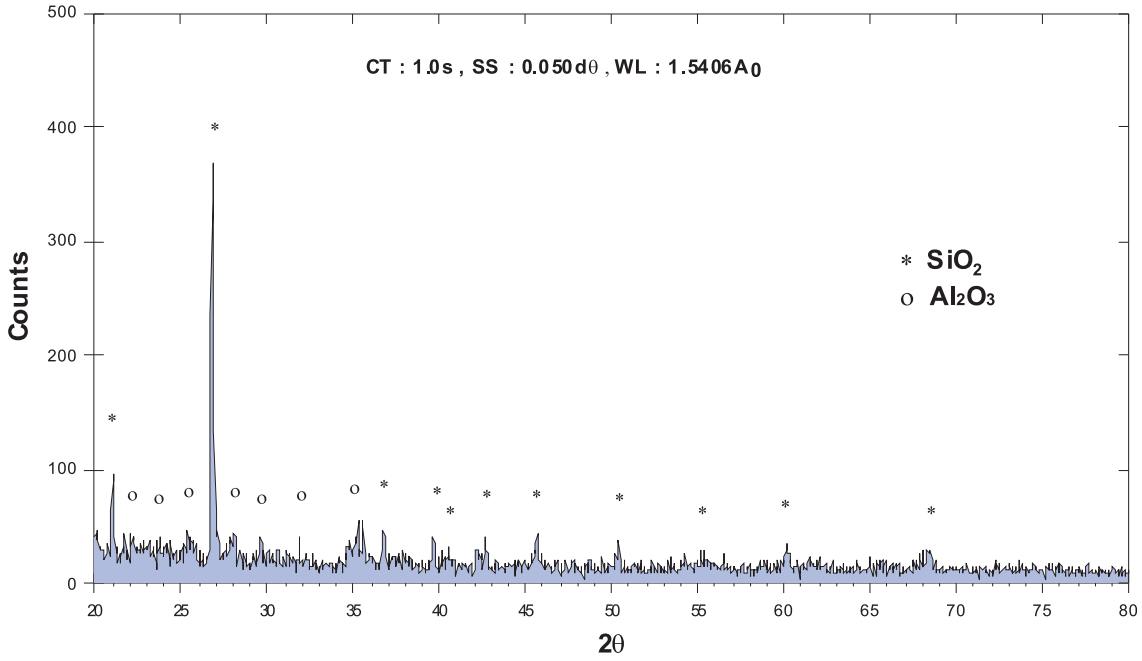

Figure 3. X-ray diffraction of marine soft silts (S-3).

silts are SiO_2 (78.1%) and Al_2O_3 (9.1%). The minor components are K_2O (4.3%), MgO (2.6%), Fe_2O_3 (2.2%), FeO (2.1%), Na_2O (1.2%), and CaO (0.4%). The results of the x-ray diffraction test are also shown in Fig. 3. The specimens were judged as weathered deposits, on the basis of the work of Wright (1981).

The particle-size-distribution curves are plotted for seabed soils taken from five locations (see Fig. 4). According to the results, the approximate contents were gravel and sand (2%), silt (45%), and clay (53%).

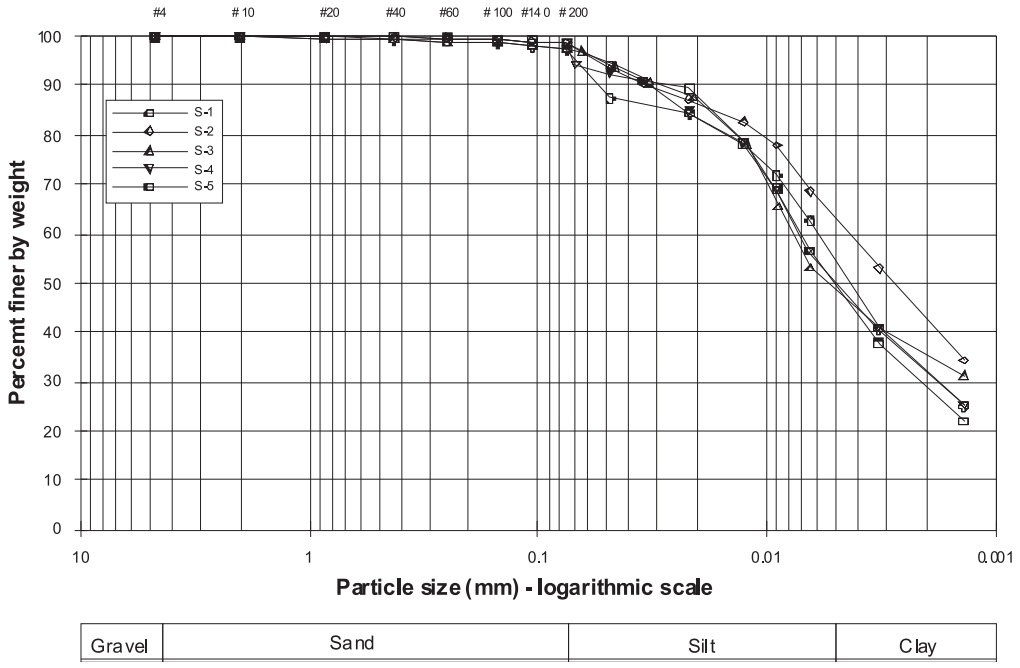

Figure 4. Particle-size-distribution curve of the soils in this experiment.

2 METHODOLOGY

A series of experiments was performed in this study, including one-dimensional consolidation and tri-axial compression tests. In order to understand the soil's basic properties, soft marine soils were prepared by a new method according to the saturated clay density, depending on the water content.

In addition, it was necessary to comprehensively analyze the soil-bearing capacity and the stability related to the slip and breakage of the foundation. The limit equilibrium method was applied to evaluate the stability of the soft ground foundation. The critical slip surface and the corresponding safety factor of the soil foundation and the relevant stress and strain of the interior slip surface can be found from the critical slip surface. The safety factor could also be found by analyzing the possible breakage mechanism.

The study analyzed the in-situ data related to stratum drilling and steel-pipe pilings. As well as the geological sampling, in-situ and laboratory experiment analysis, the density and compressibility of the soil at the soft ground were obtained from these results. The breakage of the soil layer was caused by the loading and the possible amount of settlement was evaluated by a suitable numerical model developed for the prediction of the settlement stability of soft marine ground. The results are very useful as a reference for the marine silts' stability for the planning and design of near-shore engineering.

2.1 TESTING ITEMS

The shear strength of the soft silty clay was obtained from the tri-axial test. Moreover, the specimen was prepared according to the in-situ density. Because the remolded specimen of lower unit weight was too soft, the specimen could not be set up for the tri-axial test. Therefore, a new remolding method was developed in this study. The test's controlled conditions and sets are shown in Table 1.

Table 1. Testing conditions and sets.

Test items	Dry density γ_d (t/m^3)	Consolidation Stress (kPa)	Axial pressure velocity (kPa/min)
CIU	1.00、1.05 1.10、1.15	15、20、30、40、45	list the axial stress velocity recommended by Lambe (1951)
CK_0U	1.00、1.05 1.10、1.15	30、60、90	0.5
Torvane shear test	0.88~1.04	—	—

2.2 TESTING METHODS FOR THE REMOLDED SPECIMENS

It is difficult to control the degree of saturation by using the moist temping method on marine silts. However, the shear strength was decreased with the water-content increase by applying back water pressure to the specimen in tri-axial space. The purposes of the remolded method for producing a saturated specimen were twofold: one is that the behavior of the saturated specimen was more easily controlled than the unsaturated one, and the other is that the shear strengths of the soft marine silts on the seabed were simulated.

In order to remold the very soft specimens, a new remolding method was developed in this study. The specimens were prepared using the constant volume method with dried silt clay and water contents ranging from 1.0 to 2.0%. In the specimen remolded process, a soil water content of about 200% was adopted in the test. The specimens were mixed for about 5–10 minutes at low velocity in a mixer until they became like a fluid. The soils were infiltrated into the remolded specimen instruments (7.0 cm in diameter and 20.0 cm in height) that connect with vacuum pressure. The sedimentation behavior was induced rapidly. The stresses at different steps were applied to remold the specimen gradually to reach the in-situ density, when the sedimentation stops. The remolded specimen-preparation steps are presented in Figs. 5 (a)–(d).

The C.K.C. Automatic Triaxial Test System was applied in this study, as shown in Fig.6. The test system has great advantages in stress, strain and stress path control (Chien, 2002). According to whether it is stress controlled or strain controlled, the air pressure and oil pressure can be adopted for the pressure system in the experiment. All the experimental procedures are performed through a human-computer interface to provide an easy and convenient operating environment.

As for the normal consolidated clay, the failure envelopes were calculated from the strength parameters without conducting a consolidation and drainage test. Therefore, the undrained shear strength according to half of the maximum axial differential stress $(\sigma_1 - \sigma_3)_{max}$ could be determined. When the axial strain exceeded 15%, but did not reach the maximum axial differential stress, the undrained shear strength can be defined according to 15% of the axial differential stress. Chien (2002) studied the effect of the fines content on the liquefaction strength by using the moist temping method at different relative densities and fine contents.

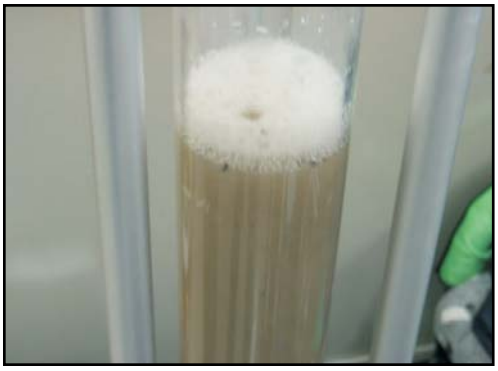

(a) The vacuity before sedimentation

(b) The specimen sedimentation

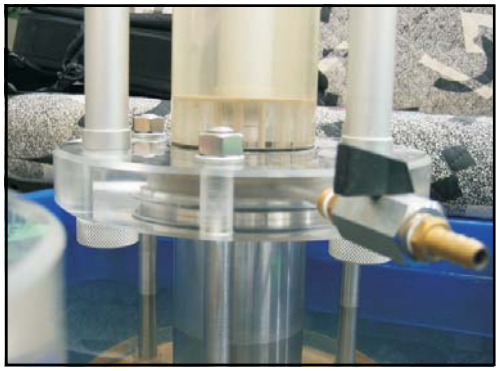

(c) Applying the steps loading

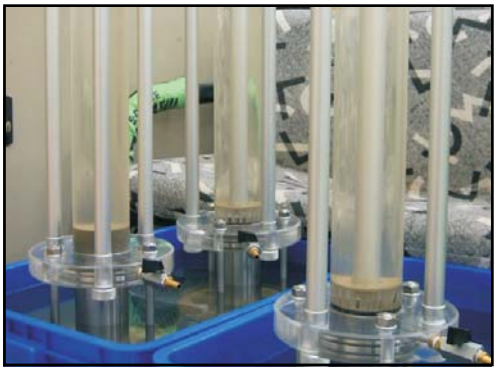

(d) Reaching the design density

Figure 5. The marine clay remold, specimen-preparation steps.

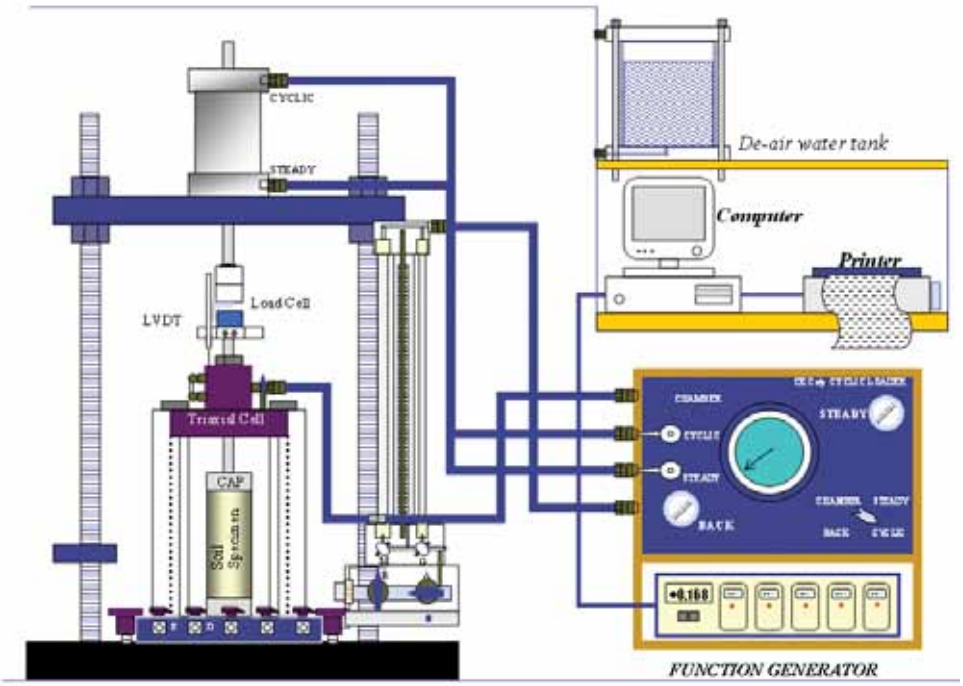

Figure 6. Sketch of the tri-axial test system.

The computer software SIGMA/W was applied to analyze the stress-strain conditions in the silt deposits, induced by the construction of the rubble breakwater structure. In order to evaluate the influence of long-term effects and excessive pore-water pressure on soft marine silts, the settlement caused by the breakwater at the Fuao Port of Ma-Zu was analyzed through a consolidation analysis and SEEP/W. The real-time consolidation and settlement caused by the rubble-mound breakwaters are predicted.

3 EXPERIMENTAL ANALYSIS AND RESULTS

3.1 DENSITY CHANGE AFTER ISOTROPIC AND K_0 CONSOLIDATION

There were four kinds of density soils selected with different initial densities for the isotropic and K_0 consolidation experiments in this study. The changes of the mean dry density (γ_d) can be obtained through different consolidation stresses, and the relationships are shown in Fig.7 and Fig. 8.

During the 45-kPa confining-pressure isotropic-consolidation process, the soil's dry density changed from an initial value of 1.10 t/m^3 to a final value of 1.22 t/m^3. This was an increase of 10.85%. Under the K_0 consolidation with the axial direction consolidation pressure ranging between 30 and 90 kPa, the soil's dry density increased from 1.7 to 13.4% when the initial dry density was 1.15 t/m^3 and from 1.9 to 14.0% when the initial dry density was 1.10 t/m^3.

The increase in the dry density was more under the isotropic consolidation (4.6 to 11.5%) than under the K_0 consolidation (1.7 to 6.4%), when the consolidation stress was equal to 30 kPa. The reason for this result was that the axial stress applied during the K_0 consolidation did not promote consolidation in the radial direction.

3.2 PORE-WATER PRESSURE INDUCED UNDER ISOTROPIC AND K_0 CONSOLIDATION

According to the isotropic and K_0 consolidation under undrained conditions, the relationship between the induced excess pore-water pressure (Δu) and the strain (ε) is shown in Fig. 9 and Fig. 10. The figures illustrate that the initial value increased gradually, and the excessive pore-water pressure increased and approached to a positive critical value as the strain increased. This phenomenon was consistent with the definition of specimen breakage by the critical state theory: the critical state was reached when the soils deformed under stress loading.

In order to further understand the induced pore-water pressure at rest, this study also discussed the relationship between the pore-water pressure ratio ($(u/\sigma'_{nc})_{max}$) and the strain (ε), where σ'_{nc} is defined as the mean consolidation stress:

$$\sigma'_{nc} = \frac{1}{3}\left(\sigma'_1 + \sigma'_2 + \sigma'_3\right) \qquad (1)$$

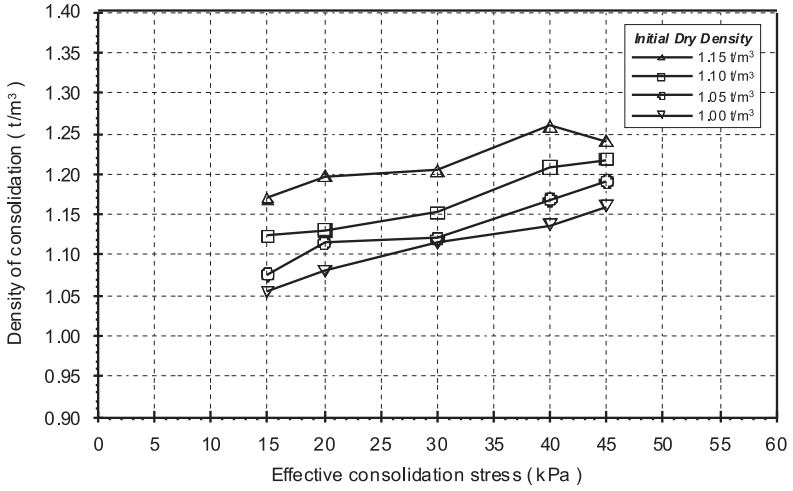

Figure 7. Dry density changes after isotropic consolidation.

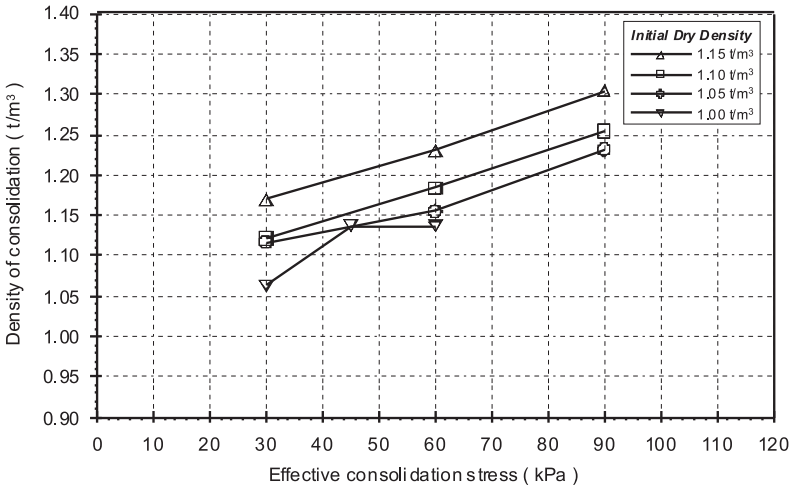

Figure 8. Dry density change after K_0 consolidation.

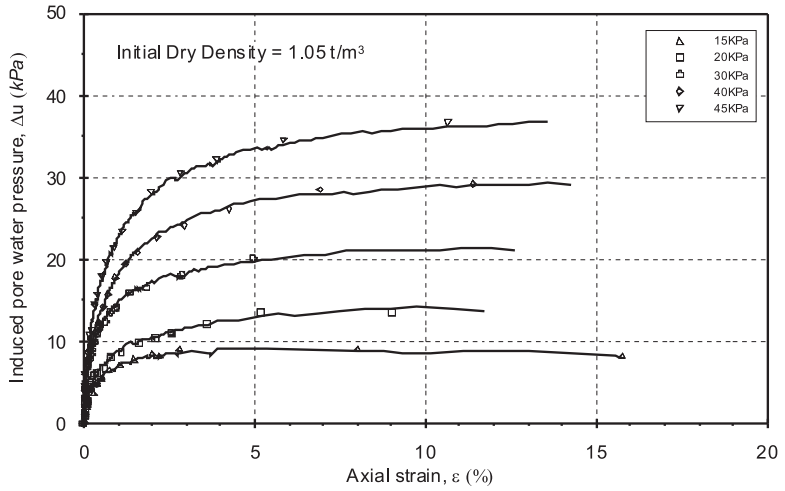

Figure 9. Relationship between Δu and ε curve for isotropic consolidation under undrained conditions.

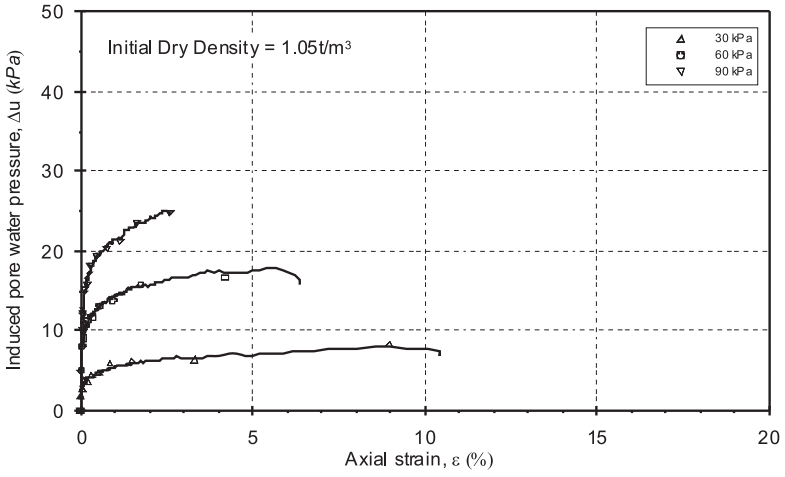

Figure 10. Relationship between Δu and ε curve for K_0 consolidation under undrained conditions.

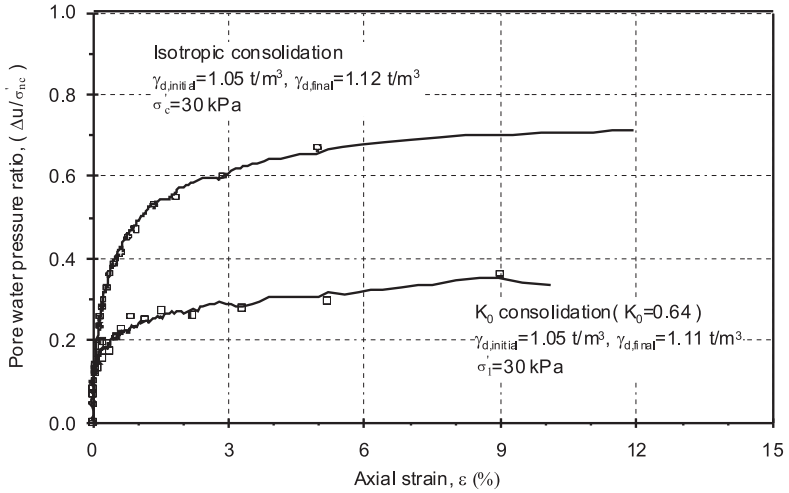

Figure 11. Comparison of the pore-water pressure model for isotropic and K_0 under undrained conditions.

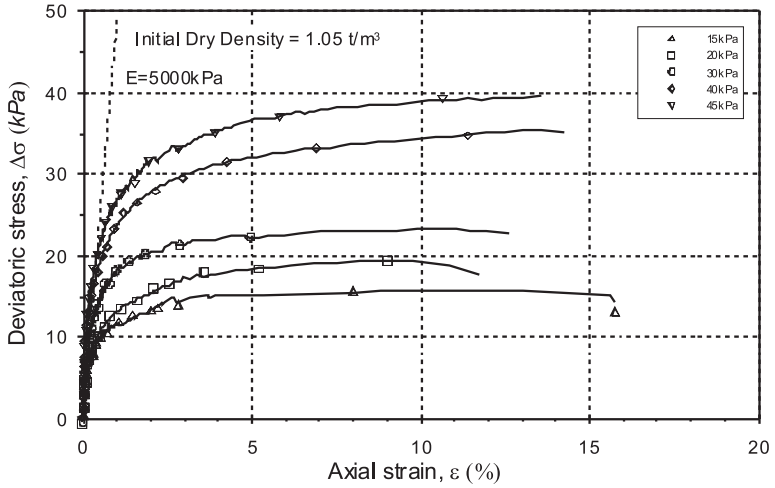

Figure 12. Relationship of $\Delta\sigma$ - ε for isotropic consolidation under undrained conditions.

The comparison of the pore-water pressure between the isotropic and K_0 consolidation processes is made in Fig. 11. The effective stress decreased gradually with the axial strain increased under static loading. However, the pore-water pressure increased more slowly during the K_0 consolidation process than during the isotropic consolidation process.

3.3 ISOTROPIC CONSOLIDATION TEST RESULTS

Fig. 12 presents the relationship between the deviatoric stress and the axial strain under isotropic with undrained conditions. For the results of the tri-axial compression testing for marine silts, the deviatoric stress increases as the confining pressure increases. Furthermore, the axial strain was plastic destruction, which, analyzed from the relationship, has no peak strength between the stress and strain.

The results of the soft marine silts experiment illustrated the total stress and effective stress path. Under the different isotropic consolidation stresses, the final stress path and the failure lines approached consistency. Furthermore, all the failure lines passed through the original point. The relationship between the different initial dry densities and the shear strength parameters is shown in Table 2.

As for the total stress strength (short term), the parameters of the effective stress strength (long term) were smaller, as shown in Fig. 13 and Fig. 14. The parameter ϕ is approximately half of the parameter ϕ'. This is consistent with the results on the consolidated clay soils reported by Holtz and Kovacs (1981).

Table 2. Shear strength parameters for soils that underwent isotropic consolidation.

Dry density (t/m^3)	c (kPa)	ϕ (°)	c' (kPa)	ϕ' (°)
1.15	0	20.37	0	43.26
1.10	0	17.21	0	35.87
1.05	0	14.73	0	25.38
1.00	0	15.36	0	30.01

3.4 K_0 CONSOLIDATION EXPERIMENT RESULTS

Due to the intrinsic anisotropy produced by the particle arrangement considered in the traditional CIU test the anisotropy produced by the K_0 consolidation ($K_0 \neq 1$) cannot be responded. Furthermore, anisotropic consolidation may affect the evaluation of the shear parameters related to the soft marine silts (Mayne, 1985). The basic mechanical behavior under K_0 consolidation is discussed below.

The experimental results (total stress and effective stress path plots) are shown for the soft marine soil in Figures 15 and 16. Under the different K_0 consolidation stresses, the initial value of the stress path lay below the state of the K_0 consolidation. Furthermore, all the failure lines passed through the coordinate origin. The relationship between the different initial dry densities and the shear strength parameters are shown in Table 3.

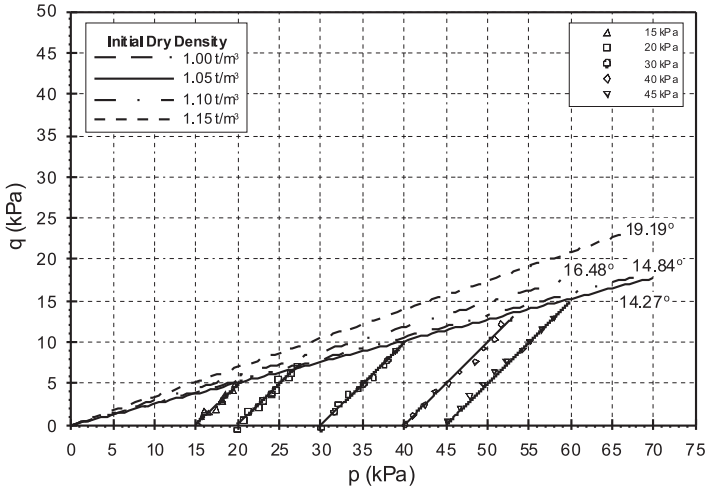

Figure 13. p - q diagram for soils that underwent isotropic consolidation.

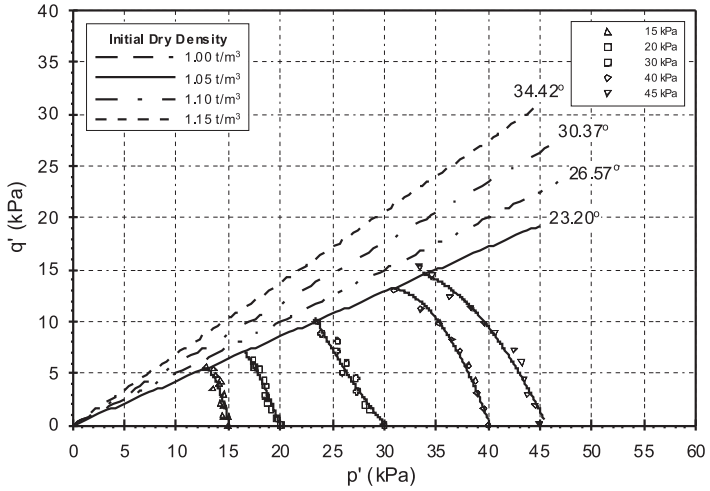

Figure 14. p' - q' diagram for soils that underwent isotropic consolidation.

Table 3. Shear strength parameters for soils that underwent K_0 consolidation.

Initial dry density (t/m^3)	c (kPa)	ϕ (°)	c' (kPa)	ϕ' (°)
1.15	0	23.58	0	34.06
1.10	0	21.71	0	30.01
1.05	0	16.26	0	23.58
1.00	0	20.49	0	26.75

According to Skempton and Sowa (1963), the shear strength of the clay can be correlated to the water content. Figure 17 presents the shear strength vs. the water content relationships for various tests performed in the present study. The following formulas describe the relationships mathematically:

$$\text{Torvane: } Su = 0.065\omega + 6.2 \qquad (2)$$

$$\text{SUU: } Su = 0.325\omega + 25.8 \qquad (3)$$

$$\text{CIU: } Su = 1.02\omega + 64.55 \qquad (4)$$

$$\text{CK}_0\text{U: } Su = 1.28\omega + 79.68 \qquad (5)$$

Where

Su: shear strength under undrained conditions (kPa)

ω: water content (%)

The marine silts were classified as extremely soft soils, based on the shear-strength results and ASTM D1586. It was also found that the shear strengths obtained from various tests were ranked as CIU > SUU > Torvane. The same ranking of shear strengths was observed in a separate study (Lin, 1988). This outcome indicates that the undrained shear strength was high for the CIU soils, since the specimens consolidated completely during the CIU test procedure. However, it was apparent that the undrained shear strengths were lower for the SUU soils, since the effective stress was zero.

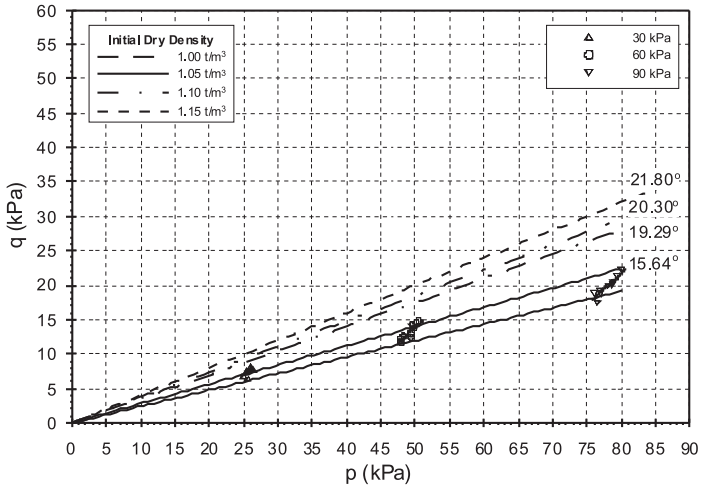

Figure 15. p - q diagram for soils that underwent K_0 consolidation.

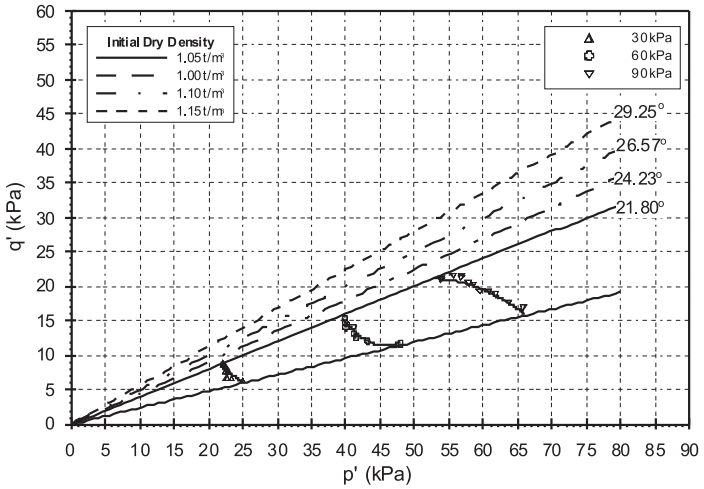

Figure 16. p' - q' diagram for soils that underwent K_0 consolidation.

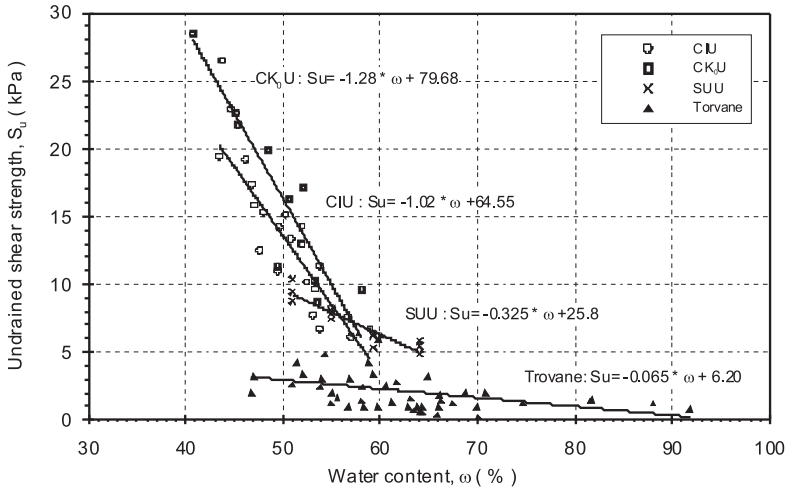

Figure 17. Undrained shear strengths resulting from different test methods.

4 NUMERICAL SIMULATION ANALYSIS

4.1 PARAMETERS FOR NUMERICAL MODE

The slope gradient was 2H:1V on the sea side and 1.5H:1V on the land side, and the crest width ranged from 18 m near shore to 21 m offshore, according to the breakwaters' design standard. For the convenience of the numerical simulation analysis, these seven sections were taken vertically across the cross-section of the structure (AA~GG). The section of the rubble-mound breakwater is shown in Fig.18 (B is the width of the breakwater crest, h is the depth of water and d is the thickness of the soft marine soils).

The marine soils were assumed to be anisotropic, elastic material during the simulation, and simplified as a single layer. Therefore, the relevant experimental parameters, such as the effective friction angle and the slope of normal consolidation line, were obtained from experimental results. According to the numerical mode requirement, the stratum condition and the soils' property parameters are shown in Table 4.

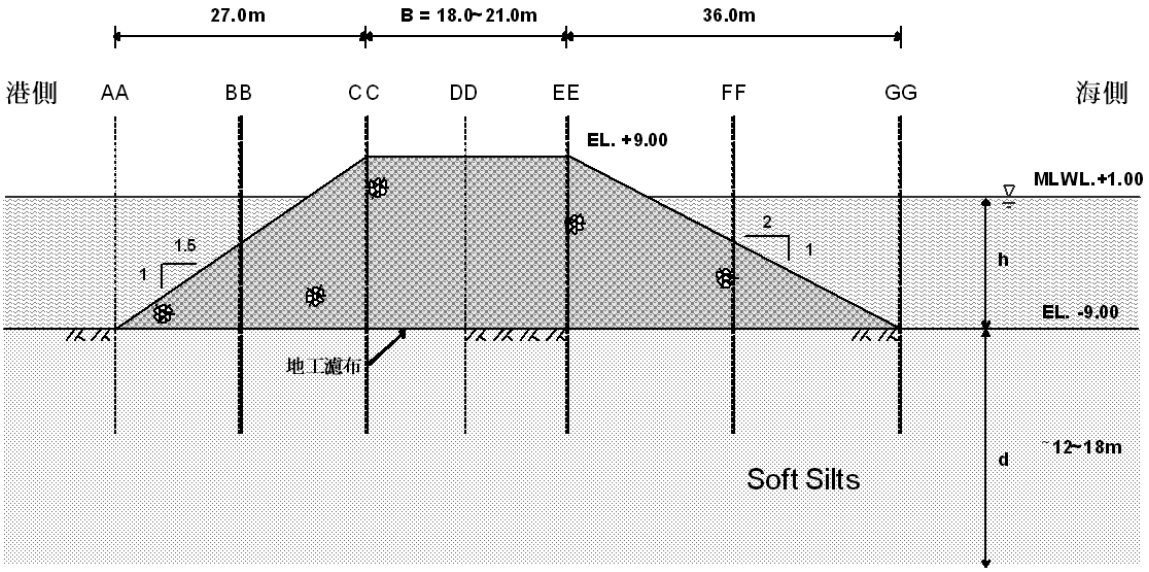

Figure 18. Sketch profile of the simplified rubble-mound breakwater.

Table 4. Parameters used in numerical simulation.

Linear Elastic	
A (pore pressure parameter)	0.78#
B (pore pressure parameter)	1.00#
E (elastic modulus)	5 MPa, 8 MPa* (Soft silt) 399 MPa (Rubble mound)
v (Poisson's ratio)	0.4 (Soft silt) 0.3 (Rubble mound)
K_0 (coefficient of earth pressure at rest)	0.60, 0.60*
γ_t (bulk unit weight)	16.4, 16.7 kN/m^3 (Soft silt) 19.6 kN/m^3 (Rubble mound)
Modified Clay	
C_c (compression index)	0.313, 0.297*
C_S (swelling index)	0.0507, 0.0496*
λ (slope of normal consolidation line)	0.136, 0.129*
κ (slope of swelling line)	0.0220, 0.0215*
ϕ' (effective friction angle)	25.38°, 35.87°*
M (slope of critical state line)	1.00, 1.46*
Γ (specific volume)	2.648, 2.527*
OCR (over consolidation ratio)	1.00
Consolidation	
k (hydraulic conductivity)	2.07×10^{-4} m/day 1.42×10^{-4} m/day*
m_v (coefficient of volume compressibility)	3.70×10^{-3} 1/kPa 3.65×10^{-3} 1/kPa*

Note:

1. The condition of filling rubbles for breakwater meets the port structures' design standard issued by the Ministry of Communications and the parameters selected from the numerical mode Jeng et al. (2001).
2. "#": These parameter values reflect the initial properties that existed at the beginning of the construction.
3. "*":These parameter values reflect the properties that existed at the end of the construction when the unit weight of the marine soils increased to 16.7 kN/m^3.

4.2 MODE PREDICTION AND RESULTS DISCUSSION. SIMULATION OF RESULTS AT DIFFERENT PHASES OF THE STRATIFIED GEO-STRUCTURE

Seven sections of the rubble-mound breakwater were analyzed to determine the maximum settlement induced during the construction steps. The settlement quantity of the soft marine silts increased with the increasing of the construction height (as shown in Fig 19). The seabed slightly up-heaved at the toe (at section GG) on the sea side. From the analysis, the largest settlement was detected near the sea-side toe (section BB), not at the core (section DD) of the breakwater, as shown in Fig. 20. The whole soft silts are stable before the construction height reached 6m, but when the height exceeded 9m, the vertical displacements were found over a large area of the soil layer and the phenomenon of upheaval was induced on the seabed. The settlement quantity increased with the increase of the thickness (h) of the soil layer and the width (B) of the breakwater. It can be concluded that the thicker soil layer may have a larger settlement.

The soft silt layers experienced lateral displacements due to the extrusion caused by the rubble-mound construction. The displacements were more obvious on the land side than on the sea side, as shown in Fig. 21.

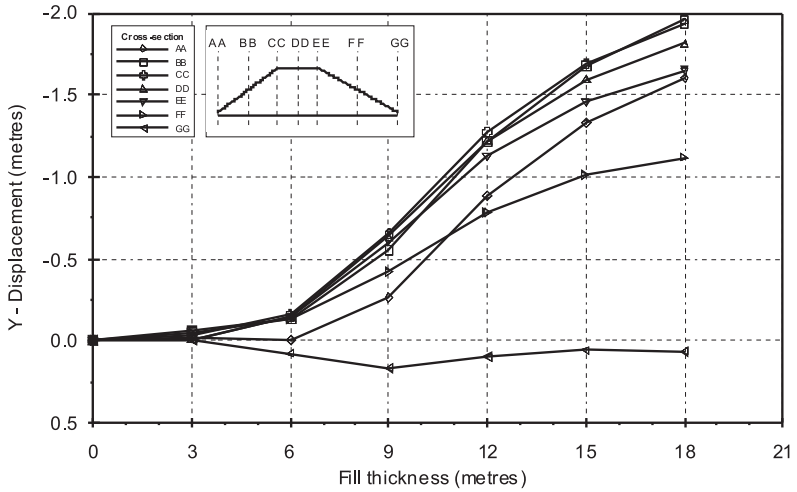

Figure 19. Settlement quantities of different sections of rubble-mound breakwaters under different construction steps.

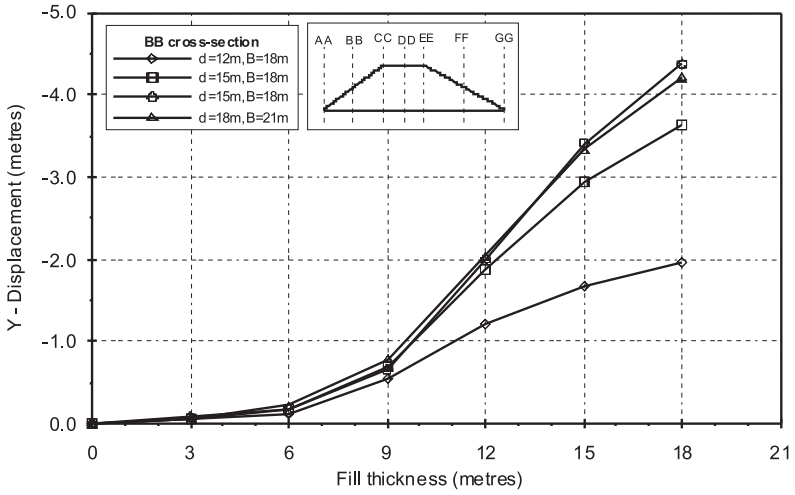

Figure 20. Thicknesses of different soil layers and the settlement quantity of rubble-mound breakwater under different construction steps.

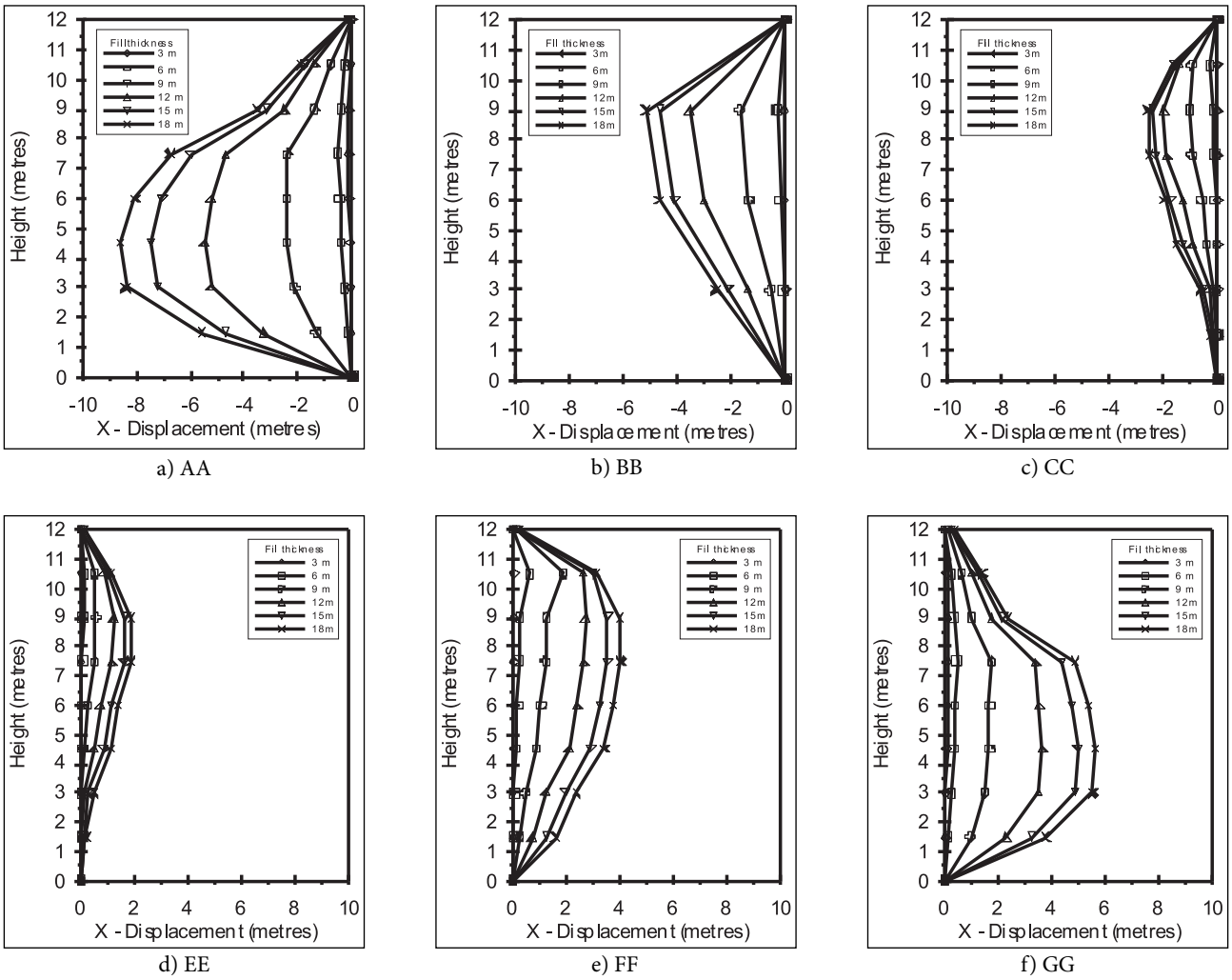

Figure 21. Side displacement of the different sections of breakwater under construction.

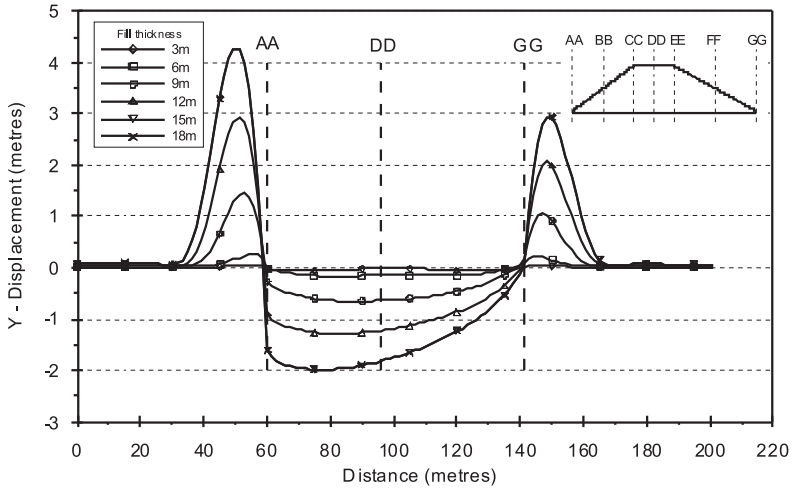

Figure 22. Settlement and upheaval of seabed under construction.

The behaviors of the seabed for filling the rubble mound under different loading were analyzed (as Fig. 22). The soft marine silts experienced larger lateral displacements under the increasing loading coming from the rubble mound, the front toe of the breakwater up-heaved due to extrusion. The area affected extended to about 40m (equivalent to four times the soil layer thickness) beyond the toe. It could be predicted that the slope of the soft marine silts suffered asymmetric loading. The bearing capacity of the soft silts cannot resist and the possible partial breakage mechanism and slip may occur.

4.3 RESULTS OF SEABED UPHEAVAL IN RUBBLE FILLING DISTANCE

When the length of the filling rubbles on in-situ reached 0k+250 m, an unreasonable settlement of the rubble-mound breakwater occurred. In order to evaluate the upheaval height caused by side displacement before the breakwater, the different seabed sites were analyzed at an interval of 120 m when filling the rubbles. The relevant stratum, mode configuration and landform before the breakwater are shown in Fig. 23 and Fig. 24.

The results of Fig.25 show that the extrusion of the seabed is most serious when the rubble filling reached 0k + 120 m. The upheaval was about 7.3 m at the other mileages of the filling rubbles and a side displacement occurred due to the construction of the breakwater. Furthermore, the slope of the stratum speeded up the slip of the slope of soil layer and the thickness of the nearshore seabed was small but a large-area upheaval occurred on it. This phenomenon coincided with the upheaval during the construction of the Baisha Port in 1995, particularly the side settlement at mileages of ok+120 m during the construction on the site.

5 CONCLUSION

In order to further discuss the disaster factors caused by marine silts, the ongoing expansion of breakwaters at the Fuao Port of Ma-Zu was chosen as the research area. A series of experiments, including one-dimensional consolidation and a tri-axial mechanical test, were performed in this study. The in-situ data related to stratum drilling and steel-pipe piling as well as geological sampling on in-situ and laboratory analyses to evaluate the breakage and possible amount of settlement of the soil layer caused by loading. A suitable numerical model was also developed for a prediction of the settlement stability of the soft marine ground in this study.

According to the isotropic and K_0 consolidation without drainage, the initial value increased gradually, and the excessive pore-water pressure increased and approached the positive critical value as the strain increased. This phenomenon was consistent with a definition of specimen breakage by critical state theory: the critical state was reached when the soils deformed under stress loading.

The relationships between different tests were *CIU* > *SUU* > *Torvane*, which coincide with the study of the shear-strength evaluation of a silts specimen under different tests (Lin, 1988). These evaluations indicated that Su values were an over estimation and may be the result of the specimen consolidated completely in the CIU test. However, it was apparent that the Su were an under estimation and the effective stresses were zero, which reduced by the specimen saturated by back pressure in the SUU test.

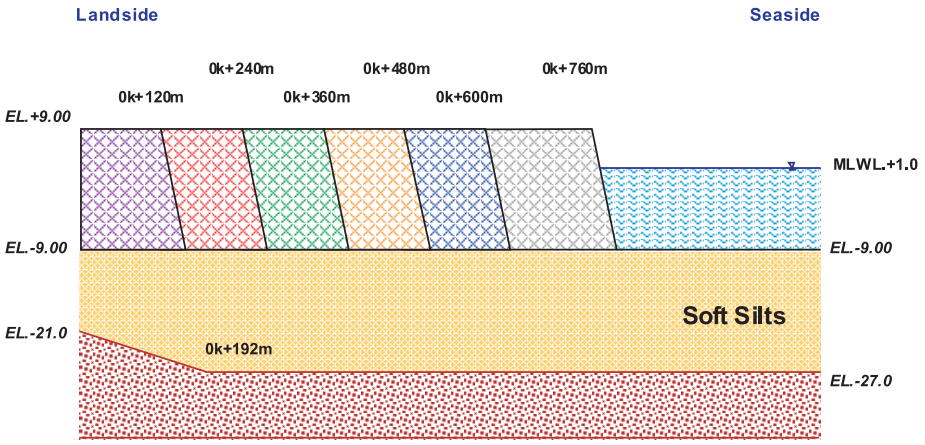

Figure 23. Landform and boundary conditions in the mode for analysis of the filling construction.

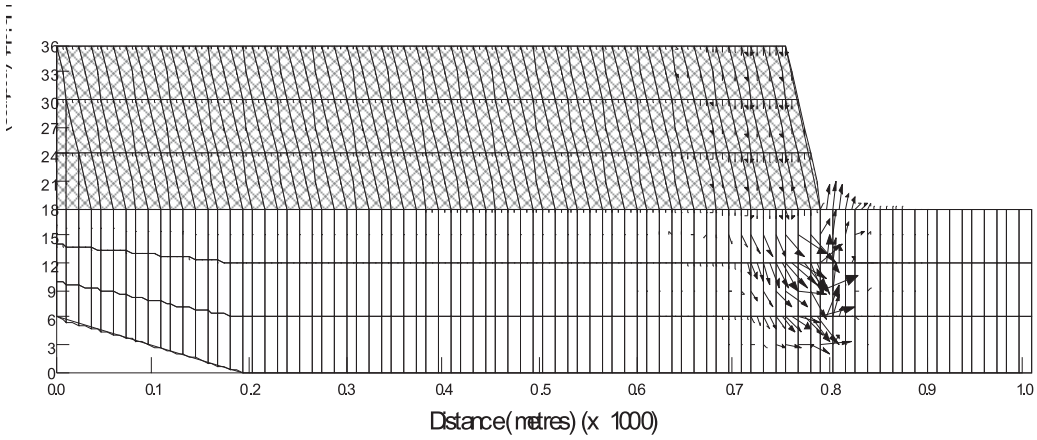

Figure 24. Landform change results of seabed before the simulation breakwater in the filling rubbles mileage.

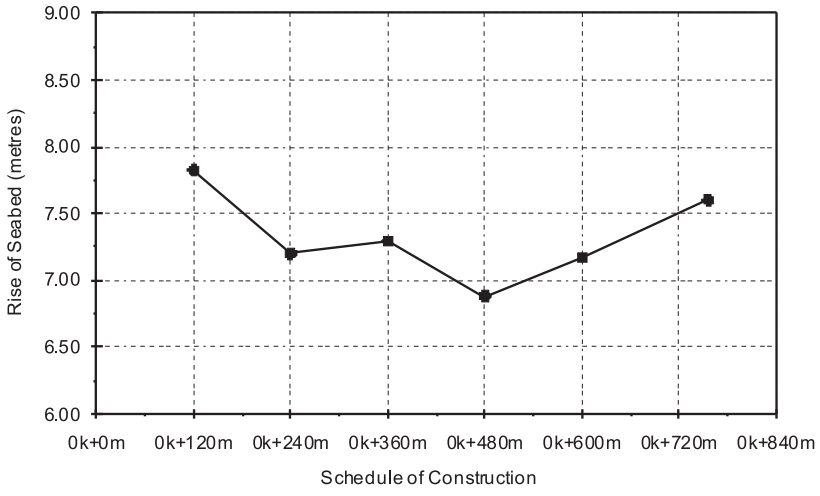

Figure 25. Rise of the front seabed in different construction mileages.

The soft marine silts at the breakwater induced displacement, greatly increasing with the filling rubble-mound loading, and then the front toe of the breakwater may experience upheaval due to extrusion. This could be predicted when the side slope of soft marine silts suffered asymmetric loading. The bearing capacity of the soft silts cannot resist and the partial breakage mechanism and slip may occur.

From the simulation results of seabed upheaval in rubble-filling mileage, the extrusion of the seabed is the most serious when the rubble filling reached 0k+120 m. The upheaval was about 7.3 m at the other construction of filling rubbles. The side displacement occurred on the near-shore due to the construction of the rubble-mound breakwater. Furthermore, the slope of stratum speeded up the slide of the slope on the soil layer. The thickness of the seabed at the near-shore was small but large-area upheaval occurred on the seabed. This phenomenon coincided with the disasters during the construction of Baisha Port in 1995, particularly the side settlement at mileages of ok+120 m during construction on the site.

REFERENCES

Atkinson, J. H., Evan J. S., Scott, C. R. (1985). Development in Microcomputer of Controlled Path Testing. *Ground Engineering*, 108, 1,15-22.

Bishop, A. W., Henkel, D. J. (1957). *The Measurement of Soil Properties in the Triaxial Test*. Edward Aronld & Co., London.

Bishop, A. W. (1958). Test Requirements for Measuring the Coefficient of Earth Pressure at Rest. *Proceedings, Conference on Earth Pressure Problems* (Brussels), Vol.1, pp.2.

Bjerrum, L. (1963). Allowable Settlement of Structure. *Proceedings of European Conf. on Soil Mech. and Found*. Eng., Weisbaden, Germany, Vol.2, pp. 35-137.

Burcharth, H. F., Frgaard, P. (1987). On the Stability of Berm Breakwater Roundheads and Trunk Erosion in Oblique Waves. Seminar on Unconventional Rubble-Mound Breakwater, Ottawa.

Chen, C. C. (2004). The Mechanical Properties of the Marine Soft Clay beneath the Near Shore Structure. Master Thesis, Dep. of Harbor and River Engineering, National Taiwan Ocean University.

Chien, Lien-Kwei, Chi-Wei Chen, Chih-Hsin Chang and Tsung-Sheng Feng (2005). Engineering behavior and settlement evaluation of cement stabilized marine clay. *Proceedings of the 27th Ocean Engineering Conference in Taiwan*, pp. 973-980.

Haykin, S. (1999). *Neural Networks*. Second ed. Prentice-Hall, Eaglewood Cliffs, NJ.

Holtz, R. D., Kovacs, W. D. (1981). *An Introduction to Geotechnical Engineering*. Prentice-Hall, Inc., Englewood Cliffs, New Jersey.

Jeng, D. S., Cha, D. H., Lin, Y. S., Hu, P. S. (2001). Wave-Induced Pore Pressure around a Composite Breakwater. *Ocean Engineering*, 28, 1413-1435.

Kim, D.H., Park, W.S. (2005). Neural network for design and reliability analysis of rubble-mound breakwaters. *Ocean Engineering*, 32 (11–12), 1332–1349.

Locat, J. (1996). On the Development of Microstructure in Collapsible soils. Lessons from the Study of Recent Sediments and Artificial Cementtation and In Genesis and Properties of Collapsible Soils by E. Derbyshire, T. Dijstra, and I. J. Smalley, Klewer Academic Publisher, Dordrecht, The Netherlands, pp.93-128.

Leonards, G. A. (1962). *Engineering Properties of Soils*. McGraw-Hill, New York, U.S.A.

Lien-kwei Chien, Tsung-shen Feng, Huo-Ping Weng and Wen-Chian Tzeng (2007). The Shear Strength and Mound Settlement of Nearshore Soft Marine Silts. *Proceedings of the 17th International Offshore and Polar Engineering Conference*, Vol. II, pp.1334-1339.

Lippmann, R.P. (1987). An introduction to computing with neural nets. *IEEE ASSP Magazine*.

Mayne, P. W. (1985). Stress Anisotropic Effects on Clay Strength. *Journal of Geotechnical Engineering*, 111, 3, 356-366

Medina, J.R., Garrido, J., Gomez-Martin, M.E., Vidal, C. (2003). Armour damage analysis using neural networks. *Proceedings of Coastal Structures, Portland*, OR, USA.

Skempton, A. W.,. Sowa, V. A (1963) The Behavior of Saturated Clays During Sampling and Testing. *Geotechnique*, 13, 4, 269-290.

Skempton, A. W. (1954). The Pore-Pressure Coefficients A and B", *Geotechnique*, 4, 143-147.

Sowers, G. F. (1962). *Shallow Foundations in Foundation Engineering*. G. A. Leonards (ed.), McGraw-Hill, New York.

Sridharan, A., Murthy, N. S., Prakash, K. (1987). Rectangular Hyperbola Method of Consolidation Analysis. *Geotechnique*, 37, 3, 355-368.

Terzaghi, K. (1925). Principles of Soil Mechanics, Determination of Permeability of Clay. *Engineering News Record*, 95, 21, 932.

Vesic, A. S. (1973). Analysis of Ultimate Loads of Soil Mechanics and Foundations. *Journal of the Soil Mechanics and Foundations Engineering*, 99, SM1, 45-73.

Whitman, R.V., Bailey, W. A. (1967). Use of Computers for Slope Stability Analysis. *Journal of the Soil Mechanics and Foundation Engineering Division*, 93, 4, 475-498.

Yagci, O., Mercan, D.E., Cigizoglu, H.K., Kabdasli, M.S. (2005). Artificial intelligence methods in breakwater damage ratio estimation. *Ocean Engineering* 32 (17/18), 2088–2106.

Yong, R. N., Sheeran, D. E. (1973). Fabric Unit Interaction and Soil Behaviour. *Proceedings of the International Symposium on Soil Structure*, Gothenburg, Sweden, 176-183.

Yong, R. N., Warkentin, B. P. (1975). *Soil Properties and Behaviour*. Elsevier Scientific Publishing Co., New York.